Influence of the Carboxy Terminus of Serum Amyloid A on Protein Oligomerization, Misfolding, and Fibril Formation

ARTICLE *in* BIOCHEMISTRY · MARCH 2012

Impact Factor: 3.02 · DOI: 10.1021/bi201903s · Source: PubMed

7 AUTHORS, INCLUDING:

Jeff Litt
University of California, Berkeley
7 PUBLICATIONS **247** CITATIONS
SEE PROFILE

Saipraveen Srinivasan
University of Texas Southwestern Medical Ce…
12 PUBLICATIONS **94** CITATIONS
SEE PROFILE

Wilfredo Colón
Rensselaer Polytechnic Institute
62 PUBLICATIONS **2,818** CITATIONS
SEE PROFILE

Published in final edited form as:
Biochemistry. 2012 April 10; 51(14): 3092–3099. doi:10.1021/bi201903s.

Influence of the Carboxy-Terminus of Serum Amyloid A On Protein Oligomerization, Misfolding, and Fibril Formation†

Sanket Patke[1], **Ronak Maheshwari**[2], **Jeffrey Litt**[1], **Saipraveen Srinivasan**[3], **J. Javier Aguilera**[3], **Wilfredo Colón**[2,3,*], and **Ravi S. Kane**[1,2,*]

[1]Department of Chemical and Biological Engineering, Rensselaer Polytechnic Institute, Troy, New York 12180

[2]Center for Biotechnology and Interdisciplinary Studies, Rensselaer Polytechnic Institute, Troy, New York 12180

[3]Department of Chemistry and Chemical Biology, Rensselaer Polytechnic Institute, Troy, New York 12180

Abstract

The fibrillar deposition of serum amyloid A (SAA) has been linked to the disease amyloid A (AA) amyloidosis. We have used the SAA isoform, SAA2.2, from the CE/J mouse strain, as a model system to explore the inherent structural and biophysical properties of SAA. Despite its non-pathogenic nature *in vivo*, SAA2.2 spontaneously forms fibrils *in vitro*, suggesting that SAA proteins are inherently amyloidogenic. However, while the importance of the amino-terminus of SAA for fibril formation has been well documented, the influence of the proline-rich and presumably disordered carboxy-terminus remains poorly understood. To clarify the inherent role of the carboxy-terminus in the oligomerization and fibrillation of SAA, we truncated the proline-rich final 13 residues of SAA2.2. We found that unlike full-length SAA2.2, the carboxy-terminal truncated SAA2.2 (SAA2.2ΔC) did not oligomerize to a hexamer or octamer, but formed a high molecular weight soluble aggregate. Moreover, SAA2.2ΔC also exhibited a pronounced decrease in the rate of fibril formation. Intriguingly, when equimolar amounts of denatured SAA2.2 and SAA2.2ΔC were mixed and allowed to refold together, the mixture formed an octamer and exhibited rapid fibrillation kinetics, similar to those for full-length SAA2.2. These results suggest that the carboxy-terminus of SAA, which is highly conserved among SAA sequences in all vertebrates, might play important structural roles, including modulating the folding, oligomerization, misfolding, and fibrillation of SAA.

Keywords

AA amyloidosis; oligomerization; Thioflavin T fluorescence; fibrils; atomic force Microscopy

Serum amyloid A (SAA), one of the major acute phase proteins, is synthesized primarily in the liver and found predominantly circulating through the plasma bound to high-density lipoproteins.[1] Variants of SAA have been found in all vertebrates investigated.[1] Although

†We acknowledge support from NIH grant R01 AG028158 to W.C. and from the P.K. Lashmet Chair Fund to R.S.K.

*To whom correspondence should be addressed: Wilfredo Colón, 110 8th St., Troy, NY, USA / Ravi S. Kane, 110 8th St., Troy, NY, USA, 12180. colonw@rpi.edu; kaner@rpi.edu. Tel: (518) 276-2515; (518) 276-2536.

SUPPORTING INFORMATION

The amino acid sequence of SAA2.2 and SAA2.2ΔC and AFM analysis of HMW soluble oligomers formed by SAA2.2ΔC (Figure S1) have been included in this section. This material is available free of cost via the internet at http://pubs.acs.org.

the detailed functions of SAA remain poorly understood, SAA appears to play an important role in functions related to inflammation, cholesterol transport, HDL metabolism, and host survival during an inflammatory response.[1, 2] An acute phase response resulting from inflammatory stimuli such as tissue injury, trauma, or infection can result in a dramatic 1000-fold increase in the plasma concentration of SAA,[3–5] which is normally present in the plasma in trace amounts.[6] Persistent high concentrations of SAA in plasma or specific tissues during the inflammatory response may result in the development of a potentially fatal disease – reactive amyloidosis or AA amyloidosis.[6–9] AA amyloidosis is characterized by the extracellular fibrillar deposition of SAA accompanied by localized cell death in organs like the liver, spleen, and kidney.[7, 10–12] SAA has also been linked to several pathological conditions including atherosclerosis, rheumatoid arthritis, cancer and Alzheimer's disease.[2, 13–16]

The fact that AA amyloidosis can be induced in mice by chronic inflammatory factors like casein, silver nitrate, or lipo-polysaccharide[2, 17] makes the mouse a good model system to study the mechanism of SAA fibrillation and pathogenesis.[18, 19] Also, since there is high sequence homology between the different variants of SAA, the mechanistic insights obtained from the mouse model may be broadly generalized and applied to other vertebrate species, including humans. Most mouse strains contain the acute phase proteins SAA1.1 and SAA2.1, but only the former is found in amyloid deposits.[20–22] Synthetic peptides corresponding to SAA1.1 residues 17–49 and 77–103, which contain heparan sulfate binding sites, were found to promote (residues 17–49)[23] or inhibit (residues 77–103)[24] the deposition of AA amyloid in a monocyte culture model for AA amyloidogenesis. In contrast to the high amyloidogenicity of SAA1.1, the CE/J mouse strain contains only one SAA isoform, SAA2.2, which does not form amyloid fibrils in vivo.[18, 19] The presence of SAA2.2 also does not protect CE/J×C57BL/6 hybrid mice from SAA1.1 amyloid deposition upon inflammation induced by casein.[25]

In spite of their different in vivo amyloidogenicities, both SAA1.1 and SAA2.2 form fibrils in vitro at 37 °C.[26–28] While SAA1.1 structural and fibrillation studies are challenging due to its poor solubility, SAA2.2, has better solubility than SAA1.1. Furthermore, the sequence of SAA1.1 differs from that of SAA2.2 at only 6 amino acid residues. Specifically, amino acid residues 6, 7, 11, 60, 63, and 101 are I, G, Q, A, S, and A in SAA1.1 and V, H, L, G, A, and D in SAA2.2, respectively. Given its higher solubility relative to SAA1.1, ability to spontaneously form fibrils in vitro at 37 °C[26–28], and very high sequence homology with SAA1.1, we have chosen SAA2.2 (the isoform produced by the CE/J mouse strain[18]) for our preliminary mechanistic studies in this work. We also note that we have used delipidated (apo) SAA2.2 for our studies. Physiologically, SAA is predominantly associated with HDL, and our studies may therefore not be relevant to the in vivo situation. However, since our goal was to probe the intrinsic role of the C-terminus in the structure and aggregation propensities of SAA, the absence of HDL was required for our in vitro studies.

Little is known about the structure of SAA2.2 beyond circular dichroism-based secondary structure analysis and algorithm-based predictions of secondary structure indicating significant alpha helix content.[27] Previous studies have shown that SAA2.2 forms a kinetically accessible octameric species upon refolding in vitro at 4 °C, which eventually is converted to a more thermodynamically stable hexamer containing a central channel.[27, 29] Although the octamer is the species formed during the first stage of refolding, the hexamer appears to be the more thermodynamically stable in vitro native state of SAA2.2.[27]

The sequence of SAA2.2 can be divided into three regions: residues 1–38, which comprise the alpha-helix-enriched N-terminal region of SAA; the central region from residues 39–86; and the proline-rich polar C-terminal region, which is believed to be solvent exposed.[27]

Most previous studies have focused on the importance of the N-terminus of SAA in fibrillation,[7, 9, 26] and the role of the carboxy-terminus in folding, oligomerization and fibrillation remains poorly understood. C-terminal truncated SAA has been found in amyloid fibrils generated during AA amyloidosis in humans; while an N-terminal fragment containing the first 76 amino acid residues predominates,[1] full-length SAA[7, 9] and other N-terminal fragments of different length have also been observed in the amyloid deposits of patients suffering from AA amyloidosis.[8, 9, 30] Therefore, it is not clear whether SAA proteolysis is a pre-requisite for amyloid deposition in vivo or a post-deposition event. It has been shown that the proteolytic removal of the C-terminus is not required for the formation of fibrils by duck SAA.[31] In addition, full length mouse SAA2.2 and SAA1.1 form fibrils in vitro under physiological-like conditions (i.e. 37 °C and pH 7.4) (reference[27] and unpublished results). Since the C-terminus is proline-rich and highly polar, it seems likely that it is not a basic component of the amyloid fibrils, thereby supporting the idea that SAA proteolysis is a post-deposition event in AA amyloidosis. In contrast, other reports suggest that the C-terminus of SAA may play a role in the pathogenesis of AA amyloidosis.[32, 33] Specifically, Magy et al. suggested that amyloid formation in AA amyloidosis involves the C-terminal processing of SAA.[32] In a recent report on the pathogenesis of AA amyloidosis, Van der Hilst suggested that C-terminal processing[7, 9, 34] and the formation of β-rich species[35] are the two prerequisites for AA amyloidosis.[33] Thus, the role of the C-terminus of SAA in AA amyloidosis is still not clear, and therefore warrants an in-depth analysis of the intrinsic role of the carboxy-terminus of lipid-free SAA in its structure, folding, and aggregation.

In this study, we investigated the influence of the carboxy-terminus on the in vitro native structure, misfolding, and fibrillation of SAA2.2. A truncated version of SAA2.2, which we call SAA2.2ΔC, was obtained by truncating 13 amino acids from the carboxy terminus of full-length SAA2.2 (103 amino acids). Truncation of full-length SAA2.2 after the ninetieth amino acid residue (i.e., before P91, see supporting information) represented the shortest truncation required to remove the proline-rich C-terminal region. While it was previously suggested that the proline-rich C-terminal residues of SAA2.2, being highly solvent exposed and most likely unstructured, were unlikely to contribute to SAA2.2 hexamerization,[27] we found that SAA2.2ΔC does not refold into hexamer or octamer, but rather forms large soluble aggregates. Also, SAA2.2ΔC exhibited slower fibrillation kinetics than SAA2.2, but formed similar protofibrils and mature fibrils. Finally, when equimolar amounts of full-length SAA2.2 and carboxy-terminal truncated SAA2.2ΔC were mixed and then allowed to refold together, the mixture formed octamers and did not exhibit slow fibrillation kinetics, further supporting an important intrinsic role for the carboxy-terminus in the in vitro folding, oligomerization, and fibrillation of SAA.

EXPERIMENTAL PROCEDURES

SAA2.2 and SAA2.2ΔC Expression and Purification

Murine SAA2.2 cDNA was cloned into a pET21-a(+) vector between the NdeI and BamHI sites and transformed into E. coli BL21 (DE3) pLysS-competent cells as described previously.[36] SAA2.2 cDNA was truncated after the ninetieth amino acid residue using a QuickChange® site-directed mutagenesis kit (Agilent, CA) and transformed into E.coli BL21 (DE3) pLysS-competent cells. The cells were grown, expressed, and lysed as described previously.[29] The protein was found to be expressed as inclusion bodies. These inclusion bodies were dissolved in cation exchange buffer (6 M Urea/20 mM sodium acetate, pH 5.6) and the lysate was loaded onto a SP Sepharose™ Fast Flow cation exchange column (GE Healthcare Biosciences) on an HPLC (Waters Corporation, MA) and eluted with cation exchange elution buffer (6 M Urea/20 mM sodium acetate/400 mM NaCl, pH 5.6) using a 10–65% salt gradient. The relevant fractions were pooled and desalted by

dialyzing them against anion exchange buffer (6 M Urea/20 mM Tris, pH 8.3). This desalted fraction was then loaded on a DE52 anion exchange column with anion exchange buffer on a HPLC (Waters Corporation, MA) and eluted with anion exchange elution buffer (6 M Urea/20 mM Tris/400 mM NaCl, pH 8.3) using a 10–65% salt gradient. The relevant fractions were pooled and concentrated via several rounds of ultrafiltration and then loaded on a HiLoad™ 16/60 Superdex™ 200 prep grade column (GE Healthcare Biosciences) pre-equilibrated with size exclusion chromatography buffer (6 M Urea/20 mM Tris/200 mM NaCl, pH 8.3) and the relevant fractions were collected and concentrated using an Amicon ultrafiltration cell. The purity of the protein was confirmed by sodium dodecyl sulfate polyacrylamide gel electrophoresis (SDS-PAGE) and electrospray ionization-mass spectroscopy. Protein concentration was determined by measuring the absorbance at 280 nm and using calculated values of the extinction coefficients.

Refolding of SAA2.2 and SAA2.2ΔC

The proteins were refolded by dialyzing against Tris buffer (20 mM Tris, pH 8.3) using a 3 kDa MWCO membrane at 4 °C. The buffer was precooled to a temperature of 4 °C before beginning dialysis. The buffer was changed after 45 min of dialysis; several additional buffer changes were carried out in the next 12 h to ensure removal of traces of urea from the solution. The dialyzed protein (~ 30 μL) was then loaded in a Superdex™ 200 10/300 GL analytical column (GE Healthcare Biosciences) at 4 °C to determine its oligomeric state. All experiments were performed using freshly refolded SAA to provide a consistent starting point for the studies.

Size Exclusion Chromatography (SEC)

Size exclusion chromatography studies on the proteins were carried out on a Superdex™ 200 10/300 GL analytical column (GE Healthcare Biosciences) using an AKTA™ purifier UPC 10 (GE Healthcare Biosciences). Molecular weight (MW) standards were used to calibrate the size exclusion chromatography column. Approximately 30–40 μL of the protein (30μM) were loaded in the column that had been pre-equilibrated with buffer (20 mM Tris/200 mM NaCl, pH 8.3, 4 °C); the elution was carried out at a flow rate of 0.5 ml/min at 4 °C. The column and the buffers were maintained at 4 °C at all times during the analysis.

Circular Dichroism (CD)

Far-UV CD spectra were recorded using a J-815 CD spectrometer (Jasco, MD). Freshly refolded protein samples were diluted to a final concentration of 30 μM using Tris buffer (20 mM Tris pH 8.3). The diluted SAA samples were loaded in a circular quartz cuvette (1 mm pathlength) and five spectra were collected from 190–240 nm for each sample with a bandwidth of 1 nm and time constant of 5 s and later averaged. The sample chamber was maintained at 4 °C during the measurements.

Dynamic Light Scattering (DLS)

The light scattering intensity of SAA2.2ΔC was measured using a DynaPro-Titan Batch dynamic light scattering instrument (Wyatt Technology Corporation, CA) and the DYNAMICS® software was used to resolve the acquisitions into well-defined distribution of hydrodynamic radii.[37] The sample chamber was maintained at 4 °C during signal acquisition. To remove any insoluble particles, the protein solutions were spun at 12000 rpm for 10 min at 4 °C prior to data acquisition. The DYNAMICS® software algorithms were used to estimate the MW of the species in the sample based on their hydrodynamic radii. The globular protein model in the DYNAMICS® program was used to estimate the MW distribution from the obtained distribution of hydrodynamic radii.

Thioflavin T (ThT) Fluorescence Assay

For the ThT fluorescence assay, a solution containing freshly refolded protein (30 μM) in Tris buffer (20 mM Tris, pH 8.3) was prepared at 4 °C and then incubated at 37 °C without agitation. At desired time intervals, 50 μL of SAA (30 μM) was first aspirated very gently and mixed with 50 μL ThT dye solution (100 μM) and 350 μL glycine NaOH buffer (50 mM glycine, pH 8.5) and the ThT fluorescence intensity at 485 nm (emission maxima) was recorded. The experimental settings used were as follows: excitation wavelength, 440 nm; emission wavelength, 485 nm; excitation bandwidth, 10 nm; emission bandwidth, 10 nm; scan time, 90 s.

SDS-PAGE

Protein samples were analyzed using 10–20% Tris-glycine SDS gels (Invitrogen). Protein bands were stained using the Coomassie blue dye.

Atomic Force Microscopy (AFM)

SAA samples at different incubation times were first diluted 10–20 fold in Tris buffer (20 mM Tris, pH 8.3). The diluted samples were applied on freshly cleaved mica and allowed to incubate for 15 min. The mica surface was then cleaned three times with filtered water and the plate was allowed to dry in air overnight. AFM images were obtained at room temperature using an Asylum Research MFP 3D AFM instrument (Asylum Research, CA), operating in tapping mode in air. Specifications of the silicon cantilevers (AC240TS, Olympus) used for AFM analysis were: spring constant, 1.8 N/m; tip radius < 10 nm; resonant frequency, 70 kHz; tip height, 14 μm; cantilever thickness, 2.8 μm.

RESULTS

Carboxy-terminal Truncated SAA Forms a High Molecular Weight Aggregate on Refolding

Full-length SAA2.2 and the truncated protein SAA2.2ΔC, having MWs of 11.67 kDa and 10.1 kDa respectively, were purified as described in the experimental procedures section. Since SAA2.2 has marginal stability at physiological temperatures,[28] we chose to refold both proteins at 4 °C, where SAA2.2 has been shown to be sufficiently stable.[29, 35] To provide a consistent starting point, we used freshly refolded proteins in experiments that compared the oligomerization and fibrillation propensities (see Experimental Procedures). Specifically, solutions of SAA2.2 or SAA2.2ΔC in a buffer containing 6 M Urea, 20 mM Tris, and 200 mM NaCl (pH 8.3) were dialysed against Tris buffer (20 mM Tris pH 8.3) over a period of 12 h with frequent buffer changes. These freshly refolded proteins were used in all the experiments described below.

We first characterized the native state of SAA2.2ΔC and compared its oligomeric state to that of full-length SAA2.2 using size exclusion chromatography (SEC). SEC data for SAA2.2 (Figure 1A) showed a dominant species (>90%) with an elution volume of 13.9 mL and a species (<10%) having an elution volume of 18.0 mL. Based on the calibration curve using MW standards, the species with an elution volume of 13.9 mL is consistent with an octameric species while the species with an elution volume of 18.0 mL represents a monomeric species. This elution profile obtained for full-length SAA2.2 agrees well with a previous report.[29] In particular, prior in vitro studies on SAA2.2 had shown that refolding of SAA2.2 results in the formation of a kinetically accessible octameric species during the initial stages of SAA refolding. In the course of 3-4 weeks at 4 °C, the octamer undergoes a gradual transformation to a hexamer.[29]

Intriguingly, SEC data for SAA2.2ΔC (Figure 1A) indicated that almost all (>95%) of SAA2.2ΔC eluted within the void volume region of the column (V_e = 7.9 ml). This result

suggests that SAA2.2ΔC does not form an octamer or hexamer, which are characteristic of the full-length SAA2.2, but instead forms high MW soluble aggregates. A small SEC peak (<5%) with an elution volume (18.1 ml) consistent with monomeric SAA2.2ΔC was also observed. Analysis of the void volume fraction by dynamic light scattering (DLS) (Figure 1B) suggests that these high MW soluble aggregates consist of a heterogeneous population of oligomers, most of which have hydrodynamic radii ranging from 7–16 nm. An oligomer with a hydrodynamic radius of 7.2 nm accounted for ~57% of the mass of the oligomer population. The DYNAMICS® MW prediction program (see Experimental Procedures) estimated that the MW of this dominant oligomer is ~750 kDa, and the MWs of the entire population of soluble aggregates range from ~700–1700 kDa (i.e. ~ 70–170 subunits). This MW range is more than the upper MW limit of the column used for analysis and would therefore explain the elution of these aggregates in the void volume. Full-length SAA2.2, on the other hand, consists primarily of an oligomer having a hydrodynamic radius of ~ 4.1 nm (Figure 1B), consistent with an octamer, as previously reported.[38] Collectively, the results obtained from SEC and DLS (Figure 1) indicate that in the absence of the carboxy-terminus, SAA2.2 did not form an octamer like full-length SAA2.2, but instead formed higher MW soluble aggregates that we will refer to as “SAA2.2ΔC aggregates”.

We also used far-UV circular dichroism (CD) spectroscopy at 4 °C to compare the secondary structures of full-length SAA2.2 and SAA2.2ΔC (Figure 1C and D). As seen in Figure 1C-D, both SAA2.2 and SAA2.2ΔC appear to have α-helical content as indicated by the two negative peaks centered around 222 nm and 208 nm. However, mean residual ellipticity values for SAA2.2ΔC are much lower than the values obtained for equimolar amounts of SAA2.2. This reduction in the ellipticity values may be a result of differential absorption flattening effects, which have been known to produce distortions in the CD spectra of large membrane proteins[39]–[41], and aggregated molecules.[42]

SAA2.2ΔC Follows Slower Fibrillation Kinetics Relative to Full-length SAA2.2

Previous studies on the fibrillation kinetics had reported that SAA2.2 is a highly amyloidogenic protein in vitro and spontaneously forms amyloid fibrils at 37 °C.[27, 28] Since in vivo amyloid deposits are complex and heterogeneous, we note that in our use of the term “amyloid” to describe the SAA fibrils formed in vitro, we refer to protein-only aggregates having a cross-beta-sheet structure. We used the Thioflavin T (ThT) binding assay to compare the fibrillation kinetics of SAA2.2 and SAA2.2ΔC (Figure 2 and Table 1). Thioflavin T is a benzothiazole dye that is characterized by enhanced fluorescence upon binding to cross-beta structures, and has been used extensively to study the fibrillation kinetics of proteins.[43–45]

To induce fibrillation, we incubated the proteins (30 μM) at 37 °C and monitored the intensity of ThT fluorescence at different time intervals. SAA2.2 aggregation was characterized by a spontaneous increase in the intensity of fluorescence (Figure 2A).[38] The ThT fluorescence intensity reached its maximum value by ~ 20 min after which there was no significant change in the fluorescence intensity. Interestingly, the rate of SAA2.2ΔC fibrillation was much slower compared to SAA2.2, and was characterized by a very gradual increase in the ThT fluorescence intensity, reaching a maximum value only after ~ 12 h (Figure 2B). The fluorescence intensities at various time points during the first 12 h fit a sigmoidal curve with an inflection point of ~ 5 h. (Figure 2B). No significant change in the ThT fluorescence values was seen after 12 h, suggesting no significant further change in the cross-β content. These results indicate that SAA2.2ΔC, which initially consists predominantly of the “SAA2.2ΔC aggregates”, follows slower fibrillation kinetics than full-length SAA2.2.

Characterization by Atomic Force Microscopy Confirms that Misfolding and Aggregation of SAA2.2ΔC Result in the Formation of SAA2.2-like Amyloid Fibrils

We monitored the misfolding and aggregation of both wild type and truncated protein by atomic force microscopy (AFM). The proteins were incubated at 37 °C and AFM samples were prepared using freshly cleaved mica (see Experimental Procedures) at different time intervals during the course of aggregation for both proteins.

As shown in Figure 3A, images obtained from samples of SAA2.2 incubated at 37 °C for 12 h showed the presence of “protofibril-like” curvilinear aggregates followed by the formation of mature fibrils in 24 h (Figure 3B). Figures 3C-D represent AFM images obtained at different time intervals during the aggregation of SAA2.2ΔC. By 24 h, small curvilinear protofibrillar aggregates started populating as seen in Figure 3C. The height of these protofibrillar aggregates was ~ 2–3 nm. Figure 3D is a representative AFM image of the samples obtained after incubating SAA2.2ΔC for 48 h at 37 °C, and it shows that SAA2.2ΔC can form mature fibrils. The height of these fibrils was also ~ 2–3 nm, similar to the height of the protofibrillar aggregates seen after 24 h and those formed by SAA2.2.

These results indicate that the aggregation of both SAA2.2ΔC and full-length SAA2.2 results in the formation of fibrils of similar height and overall morphology. This process proceeds through the formation of protofibrillar aggregates in the intermediate stage and full-length fibrils in the last stage. The rate of fibrillation, however, is considerably slower for SAA2.2ΔC than for SAA2.2. Thus, the AFM data suggests that the proline-rich C-terminus might directly affect the kinetics of SAA amyloid formation in vitro, or alternatively might play a role in protecting the lipophilic SAA2.2 against formation of non-amyloidogenic aggregates that might compete with and slow down amyloid formation.

An Equimolar Mixture of SAA2.2 and SAA2.2ΔC Forms a Mixed Octamer on Refolding that Exhibits SAA2.2-like Structure, Oligomerization, and Fibrillation Kinetics

As described previously, SAA2.2ΔC did not oligomerize into an octamer, but rather assembled into large soluble aggregates. The ability of SAA2.2ΔC to form amyloid fibrils, although at a much slower rate, indicates that the C-terminus is not intrinsically required for SAA fibril formation, but instead might play a kinetic role by limiting access to other structures that SAA might fold/aggregate into. Therefore, to further probe the role of the carboxy-terminus of SAA in its oligomerization and fibrillation, we first tested the ability of SAA2.2ΔC to oligomerize in the presence of full length SAA2.2. To that end, we mixed equimolar quantities of separately purified denatured SAA2.2ΔC and SAA2.2 (in solutions containing 6 M urea) and then refolded the mixture containing both proteins by dialysis (see Experimental Procedures). We analyzed by SEC the quaternary structure of the species formed during the initial stages of refolding of this mixture. Intriguingly, while SAA2.2 and SAA2.2ΔC refolded separately into predominantly octamers and “SAA2.2ΔC aggregates”, respectively (Figure 1 A-B), a mixture containing equimolar quantities of both proteins, refolded into a mostly octameric species with the expected SEC elution volume of 13.9 ml (Figure 4A). To determine the constituent species comprising this octamer, we used SDS-PAGE. Figure 4B is the image of the gel obtained when pure octamer, obtained by isolating the fraction corresponding to the “octamer peak” (Ve = 13.9 ml), was run on a denaturing gel. Interestingly, two separate bands were clearly visible between the 6 kDa and 16 kDa MW standards. Comparison of these two bands with those corresponding to full-length SAA2.2 and SAA2.2ΔC in adjacent lanes shows that the octamer consists of both SAA2.2 and SAA2.2ΔC. Analysis using “ImageJ” software[46, 47] indicated that both bands had very similar intensities, suggesting that the co-octamer contains equal number of subunits of SAA2.2 and SAA2.2ΔC. We next characterized the secondary structure of this “co-oligomer” by far-UV CD spectroscopy. As seen in Figure 4C, the “co-oligomer” was rich in

α-helical content, which was evident from the two negative peaks at 222 and 208 nm. The observation that SAA2.2ΔC cannot form octamers in isolation (Figure 1A-B), but can form octamers in the presence of full length SAA2.2 confirms the importance of the carboxy-terminus of SAA for in vitro native state oligomerization. Furthermore, SAA2.2ΔC's ability to form mixed octamers with SAA2.2 suggests that the C-terminus is not structurally essential for octamer formation, and might instead play a role in stabilizing the octamer or providing it kinetic accessibility early in folding/oligomerization.

Next, we studied the aggregation kinetics of the "co-oligomer" by using the ThT fluorescence assay. The "co-oligomer" aggregation was characterized by a rapid increase in the ThT fluorescence intensity, suggesting spontaneous conversion of the α-helical "co-oligomer" to cross-β rich aggregates (Figure 4D). In fact, the ThT fluorescence spectrum displayed no observable lag time, and the fluorescence reached its maximum value by ~ 20 min. This trend of fast fibrillation kinetics exhibited by the "co-oligomer", is similar to that for full length SAA2.2 (Figure 2A) but significantly different from the much slower profile displayed by SAA2.2ΔC alone. The faster fibrillation kinetics of SAA2.2 and the "co-oligomer" suggests that the octamer provides a more direct access to the fibril formation pathway than the larger "SAA2.2ΔC aggregates".

DISCUSSION

A better understanding of the biological and pathological roles of the carboxy-terminus of SAA will require elucidating the intrinsic influence of this polar and proline-rich region in the folding, oligomerization, and fibril formation of non-pathological and pathological SAA isoforms. Although the carboxy-terminus of SAA seems likely to be intrinsically disordered, our results suggest that it nevertheless plays an important role in determining the in vitro oligomeric state of SAA2.2 (Figure 1). However, our co-refolding experiments suggest that the C-terminus of SAA does not play a direct structural role in octamer oligomerization, but rather seems to facilitate octamer formation by inhibiting the formation of other structures, The recruitment of SAA2.2ΔC by SAA2.2 early in folding to form a co-octamer with equal amounts of both SAAs, suggests that this recruitment (i.e. SAA2.2-SAA2.2ΔC interaction) is efficient and may occur at the level of dimerization.

Comparison of the fibrillation kinetics of SAA2.2 and SAA2.2ΔC using the ThT fluorescence assay revealed that the truncation of the carboxy-terminus of SAA2.2 significantly reduces its rate of fibrillation. Nevertheless, AFM results show that both proteins followed similar fibrillation pathways and ultimately formed amyloid fibrils with similar morphologies. These results suggest that the proline-rich C-terminus plays a kinetic role in SAA2.2 fibril formation in vitro, instead of being an integral part of the fibril structure. Plausible reasons for the long lag phase of SAA2.2ΔC include slow dissociation of the SAA2.2ΔC aggregate, slow rate of α-helix to β-sheet misfolding, and formation of off-pathway oligomers competing with the formation of on-pathway amyloidogenic oligomers.

The ability of SAA to "rescue" SAA2.2ΔC early in folding from a pathway leading to high MW aggregates, suggests that the C-terminus assists native folding and oligomerization by inhibiting misfolding and aggregation into other structures. It is also worth noting that the C-terminus of SAA contains a heparan sulfate binding site,[48] and previous studies have shown that heparan sulfate may facilitate amyloid fibril formation.[24, 49, 50] Thus, the C-terminus of SAA, which is also highly conserved among SAA sequences in all vertebrates, might play important structural roles, including modulating the folding, oligomerization, and fibrillation of SAA.

Several studies on different amyloid proteins have suggested that early intermediates (nonnative oligomers) or "protofibrils" in the aggregation pathway of amyloid proteins may be the primary toxic species and that fibril formation might be a defensive mechanism to minimize toxicity.[51–55] Owing to its slower rate of fibrillation, SAA2.2ΔC aggregates exist as spherical aggregates and "protofibrillar" aggregates for a longer period of time as compared to SAA2.2. In future work, we will compare the toxicity of the intermediate aggregates and protofibrils formed by carboxy-terminal truncated and full-length SAA2.2 and SAA1.1. These forthcoming studies with the in vivo pathogenic isoform SAA1.1 and other pathogenic SAAs (e.g., human SAAs) might help illuminate the toxic species and the significance of the carboxy-terminus processing in AA amyloidosis.

Supplementary Material

Refer to Web version on PubMed Central for supplementary material.

Acknowledgments

We would like to acknowledge Dr. Dmitri Zagorevsky for assistance with mass-spectroscopy analysis and Dr. Joel Morgan for his assistance with HPLC and DLS.

Abbreviations

SAA	Serum amyloid A
SAA2.2ΔC	carboxy-terminal truncated SAA
AA	Amyloid A
CD	circular dichroism
DLS	dynamic light scattering
SEC	size exclusion chromatography
ThT	Thioflavin T
Tris	tris(hydroxymethyl)aminomethane
MW	molecular weight

REFERENCES

1. Uhlar CM, Whitehead AS. Serum amyloid A, the major vertebrate acute-phase reactant. Eur J Biochem. 1999; 265:501–523. [PubMed: 10504381]
2. McAdam KP, Sipe JD. Murine model for human secondary amyloidosis: genetic variability of the acute-phase serum protein SAA response to endotoxins and casein. J Exp Med. 1976; 144:1121–1127. [PubMed: 978136]
3. Hoffman JS, Benditt EP. Changes in high density lipoprotein content following endotoxin administration in the mouse. Formation of serum amyloid protein-rich subfractions. J Biol Chem. 1982; 257:10510–10517. [PubMed: 7107614]
4. Kushner I. The Phenomenon of the Acute Phase Response. Ann N Y Acad Sci. 1982; 389:39–48. [PubMed: 7046585]
5. Marhaug G. 3 Assays for the Characterization and Quantitation of Human-Serum Amyloid-A. Scand J Immunol. 1983; 18:329–338. [PubMed: 6417768]
6. Gillmore JD, Lovat LB, Persey MR, Pepys MB, Hawkins PN. Amyloid load and clinical outcome in AA amyloidosis in relation to circulating concentration of serum amyloid A protein. Lancet. 2001; 358:24–29. [PubMed: 11454373]

7. Husebekk A, Skogen B, Husby G, Marhaug G. Transformation of amyloid precursor SAA to protein AA and incorporation in amyloid fibrils in vivo. Scand J Immunol. 1985; 21:283–287. [PubMed: 3922050]
8. Westermark GT, Sletten K, Westermark P. Massive Vascular Aa-Amyloidosis - a Histologically and Biochemically Distinctive Subtype of Reactive Systemic Amyloidosis. Scand J Immunol. 1989; 30:605–613. [PubMed: 2587936]
9. Rocken C, Shakespeare A. Pathology, diagnosis and pathogenesis of AA amyloidosis. Virchows Arch. 2002; 440:111–122. [PubMed: 11964039]
10. Gertz, MA.; Kyle, RA. Secondary Systemic Amyloidosis (Aa) - Response and Survival in 64 Patients; Amyloid Amyloidosis Int Symp Amyloidosis, 6 th; 1991. p. 817-820.
11. Hamed G, Heffess CS, Shmookler BM, Wenig BM. Amyloid Goiter - a Clinicopathological Study of 14 Cases and Review of the Literature. Am J Clin Pathol. 1995; 104:306–312. [PubMed: 7677120]
12. Tuglular S, Yalcinkaya F, Paydas S, Oner A, Utas C, Bozfakioglu S, Ataman R, Akpolat T, Ok E, Sen S, Dusunsel R, Evrenkaya R, Akoglu E. A retrospective analysis for aetiology and clinical findings of 287 secondary amyloidosis cases in Turkey. Nephrol Dial Transplant. 2002; 17:2003–2005. [PubMed: 12401861]
13. Husby G, Marhaug G, Sletten K. Amyloid A in systemic amyloidosis associated with cancer. Cancer Res. 1982; 42:1600–1603. [PubMed: 7060030]
14. Chung TF, Sipe JD, McKee A, Fine RE, Schreiber BM, Liang JS, Johnson RJ. Serum amyloid A in Alzheimer's disease brain is predominantly localized to myelin sheaths and axonal membrane. Amyloid. 2000; 7:105–110. [PubMed: 10842712]
15. Meek RL, Urielishoval S, Benditt EP. Expression of Apolipoprotein Serum Amyloid-a Messenger-Rna in Human Atherosclerotic Lesions and Cultured Vascular Cells - Implications for Serum Amyloid-a Function. Proc Natl Acad Sci USA. 1994; 91:3186–3190. [PubMed: 8159722]
16. Liang JS, Sloane JA, Wells JM, Abraham CR, Fine RE, Sipe JD. Evidence for local production of acute phase response apolipoprotein serum amyloid A in Alzheimer's disease brain. Neurosci Lett. 1997; 225:73–76. [PubMed: 9147377]
17. Skinner M, Shirahama T, Benson MD, Cohen AS. Murine Amyloid Protein Aa in Casein-Induced Experimental Amyloidosis. Lab Invest. 1977; 36:420–427. [PubMed: 403374]
18. Sipe JD, Carreras I, Gonnerman WA, Cathcart ES, Debeer MC, Debeer FC. Characterization of the Inbred Ce/J Mouse Strain as Amyloid Resistant. Am J Pathol. 1993; 143:1480–1485. [PubMed: 7901995]
19. Kindy MS, de Beer FC. A mouse model for serum amyloid A amyloidosis. Methods Enzymol. 1999; 309:701–716. [PubMed: 10507056]
20. Hoffman JS, Ericsson LH, Eriksen N, Walsh KA, Benditt EP. Murine tissue amyloid protein AA. NH2-terminal sequence identity with only one of two serum amyloid protein (ApoSAA) gene products. J Exp Med. 1984; 159:641–646. [PubMed: 6693836]
21. Meek RL, Hoffman JS, Benditt EP. Amyloidogenesis - One Serum Amyloid-a Isotype Is Selectively Removed from the Circulation. J Exp Med. 1986; 163:499–510. [PubMed: 3950541]
22. Shiroo M, Kawahara E, Nakanishi I, Migita S. Specific deposition of serum amyloid A protein 2 in the mouse. Scand J Immunol. 1987; 26:709–716. [PubMed: 3423740]
23. Elimova E, Kisilevsky R, Ancsin JB. Heparan sulfate promotes the aggregation of HDL-associated serum amyloid A: evidence for a proamyloidogenic histidine molecular switch. FASEB J. 2009; 23:3436–3448. [PubMed: 19549924]
24. Ancsin JB, Elimova E, Kisilevsky R, Szarek WA. Amyloidogenesis recapitulated in cell culture: a peptide inhibitor provides direct evidence for the role of heparan sulfate and suggests a new treatment strategy. Faseb Journal. 2004; 18:1749–1751. [PubMed: 15345688]
25. Wang L, Liepnieks JJ, Benson MD, Kluve-Beckerman B. Expression of SAA and amyloidogenesis in congenic mice of CE/J and C57BL/6 strains. Amyloid. 2000; 7:26–31. [PubMed: 10842702]
26. Westermark GT, Engstrom U, Westermark P. The N-Terminal Segment of Protein Aa Determines Its Fibrillogenic Property. Biochem Biophys Res Commun. 1992; 182:27–33. [PubMed: 1731787]

27. Wang LM, Lashuel HA, Walz T, Colon W. Murine apolipoprotein serum amyloid A in solution forms a hexamer containing a central channel. Proc Natl Acad Sci USA. 2002; 99:15947–15952. [PubMed: 12456883]
28. Wang L, Lashuel HA, Colon W. From hexamer to amyloid: marginal stability of apolipoprotein SAA2.2 leads to in vitro fibril formation at physiological temperature. Amyloid. 2005; 12:139–148. [PubMed: 16194868]
29. Wang Y, Srinivasan S, Ye ZQ, Aguilera JJ, Lopez MM, Colon W. Serum amyloid A 2.2 refolds into a octameric oligomer that slowly converts to a more stable hexamer. Biochemical and Biophysical Research Communications. 2011; 407:725–729. [PubMed: 21439938]
30. Stix B, Kahne T, Sletten K, Raynes J, Roessner A, Rocken C. Proteolysis of AA amyloid fibril proteins by matrix metalloproteinases-1,-2, and-3. Am J Pathol. 2001; 159:561–570. [PubMed: 11485914]
31. Ericsson LH, Eriksen N, Walsh KA, Benditt EP. Primary structure of duck amyloid protein A. The form deposited in tissues may be identical to its serum precursor. FEBS Lett. 1987; 218:11–16. [PubMed: 3109944]
32. Magy N, Benson MD, Liepnieks JJ, Kluve-Beckerman B. Cellular events associated with the initial phase of AA amyloidogenesis: insights from a human monocyte model. Amyloid. 2007; 14:51–63. [PubMed: 17453625]
33. van der Hilst J. Recent Insights into the Pathogenesis of Type AA Amyloidosis. TheScientificWorldJournal. 2011; 11:641–650.
34. Husby G, Marhaug G, Dowton B, Sletten K, Sipe JD. Serum Amyloid-a (Saa) - Biochemistry, Genetics and the Pathogenesis of Aa Amyloidosis. Amyloid. 1994; 1:119–137.
35. Zhuqiu, Y. Chemistry and Chemical Biology. Troy: Rensselaer Polytechnic Institute; 2008. Structural and mechanistic studies of amyloid fibril formation by serum amyloid A 2.2.
36. Liang J, Elliott-Bryant R, Hajri T, Sipe JD, Cathcart ES. A unique amyloidogenic apolipoprotein serum amyloid A (apoSAA) isoform expressed by the amyloid resistant CE/J mouse strain exhibits higher affinity for macrophages than apoSAA1 and apoSAA2 expressed by amyloid susceptible CBA/J mice. Biochim Biophys Acta. 1998; 1394:121–126. [PubMed: 9767146]
37. Jain S, Udgaonkar JB. Evidence for Stepwise Formation of Amyloid Fibrils by the Mouse Prion Protein. J Mol Biol. 2008; 382:1228–1241. [PubMed: 18687339]
38. Yun, W. Chemistry and Chemical Biology. Troy: Rennselaer Polytechnic Institute; 2010. Investigating the structural and amyloidogenic properties of murine SAA isoforms to explore the molecular basis of amyloid A amyloidosis; p. 126
39. Wallace BA, Mao D. Circular-Dichroism Analyses of Membrane-Proteins - an Examination of Differential Light-Scattering and Absorption Flattening Effects in Large Membrane-Vesicles and Membrane Sheets. Analytical Biochemistry. 1984; 142:317–328. [PubMed: 6528970]
40. Wallace BA, Teeters CL. Differential absorption flattening optical effects are significant in the circular dichroism spectra of large membrane fragments. Biochemistry. 1987; 26:65–70. [PubMed: 3828309]
41. Ji TH, Urry DW. Correlation of Light Scattering and Absorption Flattening Effects with Distortions in Circular Dichroism Patterns of Mitochondrial Membrane Fragments. Biochemical and Biophysical Research Communications. 1969; 34:404–411. [PubMed: 5776388]
42. Castiglioni E, Abbate S, Longhi G, Gangemi R, Lauceri R, Purrello R. Absorption flattening as one cause of distortion of circular dichroism spectra of Delta-RuPhen(3) center dot H2TPPS complex. Chirality. 2007; 19:642–646. [PubMed: 17568427]
43. Khurana R, Coleman C, Ionescu-Zanetti C, Carter SA, Krishna V, Grover RK, Roy R, Singh S. Mechanism of thioflavin T binding to amyloid fibrils. J Struct Biol. 2005; 151:229–238. [PubMed: 16125973]
44. Naiki H, Higuchi K, Hosokawa M, Takeda T. Fluorometric-Determination of Amyloid Fibrils Invitro Using the Fluorescent Dye, Thioflavine-T. Anal Biochem. 1989; 177:244–249. [PubMed: 2729542]
45. Biancalana M, Koide S. Molecular mechanism of Thioflavin-T binding to amyloid fibrils. Biochim Biophys Acta. 1804:1405–1412. [PubMed: 20399286]
46. Rasband WS. ImageJ. 1997–2005

47. Abramoff MD, Magelhaes PJ, Ram SJ. Image Processing with ImageJ. Biophotonics Int. 2004; 11:36–42.

48. Ancsin JB, Kisilevsky R. The heparin/heparan sulfate-binding site on apo-serum amyloid A. Implications for the therapeutic intervention of amyloidosis. J Biol Chem. 1999; 274:7172–7181. [PubMed: 10066777]

49. Snow AD, Kisilevsky R. Temporal Relationship between Glycosaminoglycan Accumulation and Amyloid Deposition during Experimental Amyloidosis - a Histochemical-Study. Laboratory Investigation. 1985; 53:37–44. [PubMed: 2409350]

50. Li JP, Galvis MLE, Gong F, Zhang X, Zcharia E, Metzger S, Vloclavsky I, Kisilevsky R, Lindahl U. In vivo fragmentation of heparan sulfate by heparanase overexpression renders mice resistant to amyloid protein A amyloidosis. Proceedings of the National Academy of Sciences of the United States of America. 2005; 102:6473–6477. [PubMed: 15843464]

51. Jan A, Hartley DM, Lashuel HA. Preparation and characterization of toxic A beta aggregates for structural and functional studies in Alzheimer's disease research. Nat Protoc. 2010; 5:1186–1209. [PubMed: 20539293]

52. McLean CA, Cherny RA, Fraser FW, Fuller SJ, Smith MJ, Beyreuther K, Bush AI, Masters CL. Soluble pool of Abeta amyloid as a determinant of severity of neurodegeneration in Alzheimer's disease. Ann Neurol. 1999; 46:860–866. [PubMed: 10589538]

53. Caughey B, Lansbury PT. Protofibrils, pores, fibrils, neurodegeneration: Separating the responsible protein aggregates from the innocent bystanders. Annu Rev Neurosci. 2003; 26:267–298. [PubMed: 12704221]

54. Chiti F, Dobson CM. Protein misfolding, functional amyloid, human disease. Annu Rev Biochem. 2006; 75:333–366. [PubMed: 16756495]

55. Kayed R, Head E, Thompson JL, McIntire TM, Milton SC, Cotman CW, Glabe CG. Common Structure of Soluble Amyloid Oligomers Implies Common Mechanism of Pathogenesis. Science. 2003; 300:486–489. [PubMed: 12702875]

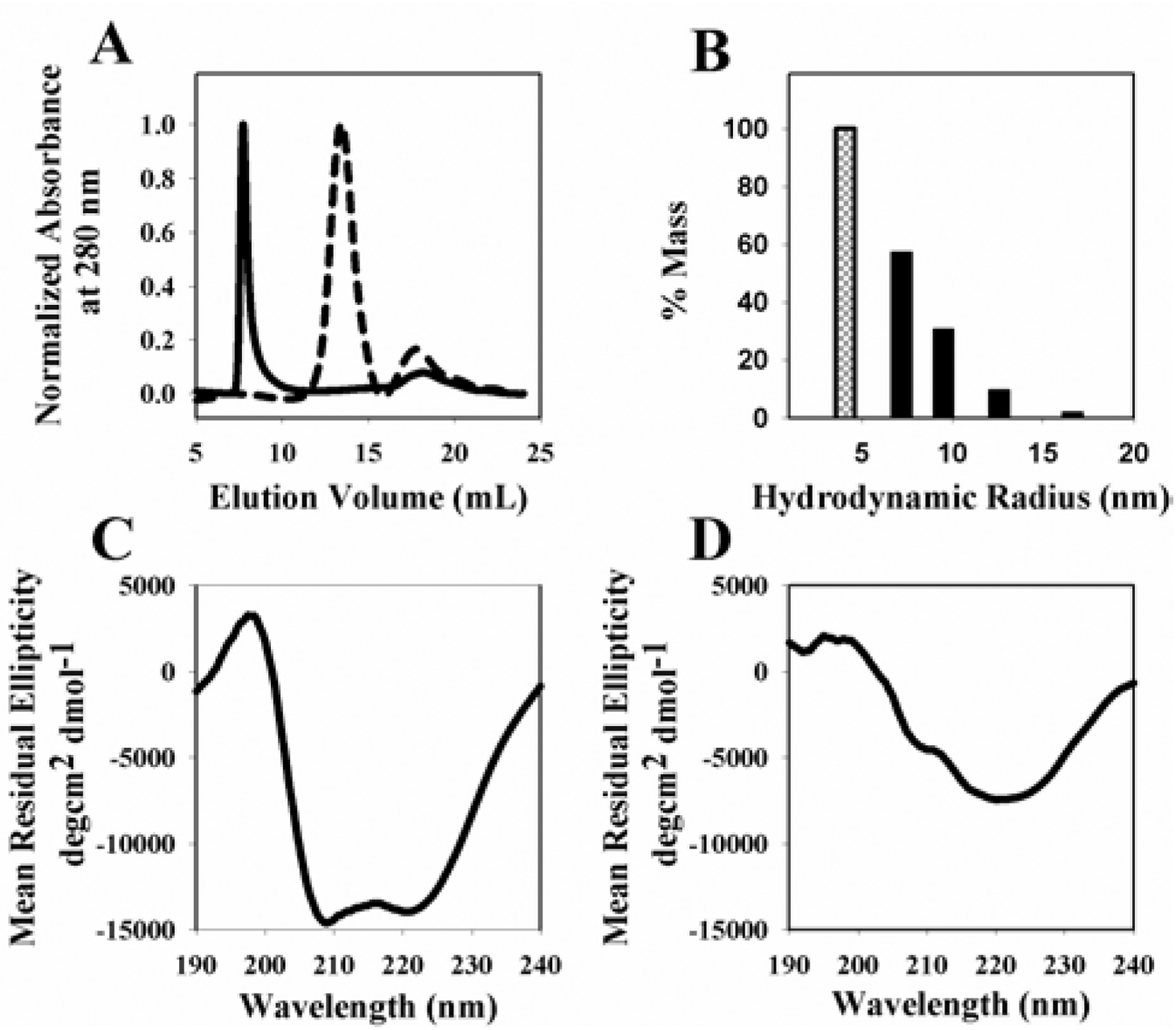

Figure 1.

Characterization of SAA2.2 and SAA2.2ΔC by SEC, DLS and Far UV-CD. (A) SEC elution profiles of SAA2.2 (– –) and SAA2.2ΔC (—). (B) Distribution of the hydrodynamic radii of SAA2.2 (☒) and SAA2.2ΔC (■) as measured by dynamic light scattering. Percent mass is plotted against the hydrodynamic radius. (C) and (D) Far UV-CD spectra of SAA2.2 and SAA2.2ΔC respectively. The concentration of protein was 30 μM. SEC, DLS and CD experiments were performed at 4 °C.

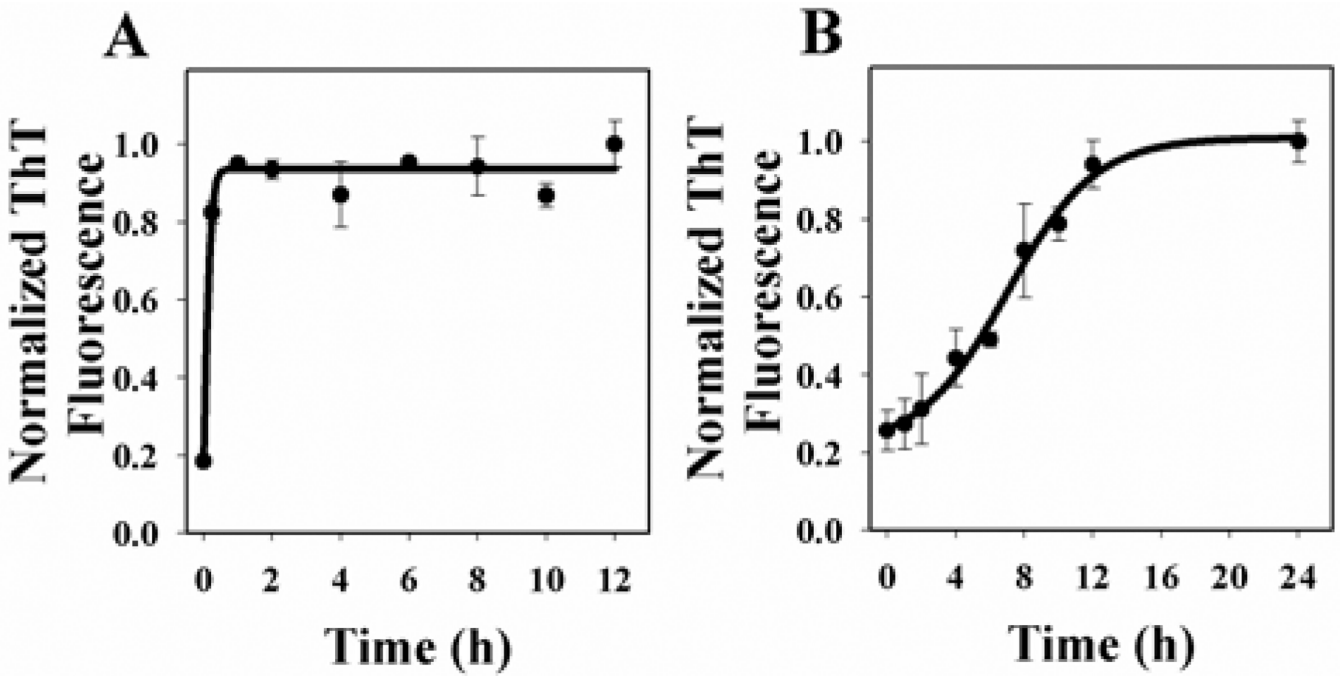

Figure 2.

Characterization of the aggregation of SAA2.2 and SAA2.2ΔC by the ThT fluorescence assay. ThT fluorescence intensity as a function of time to monitor fibril formation for (A) SAA2.2 and (B) SAA2.2ΔC. The concentration of protein was 30 μM. ThT fluorescence intensities were recorded by incubating the samples at 37 °C.

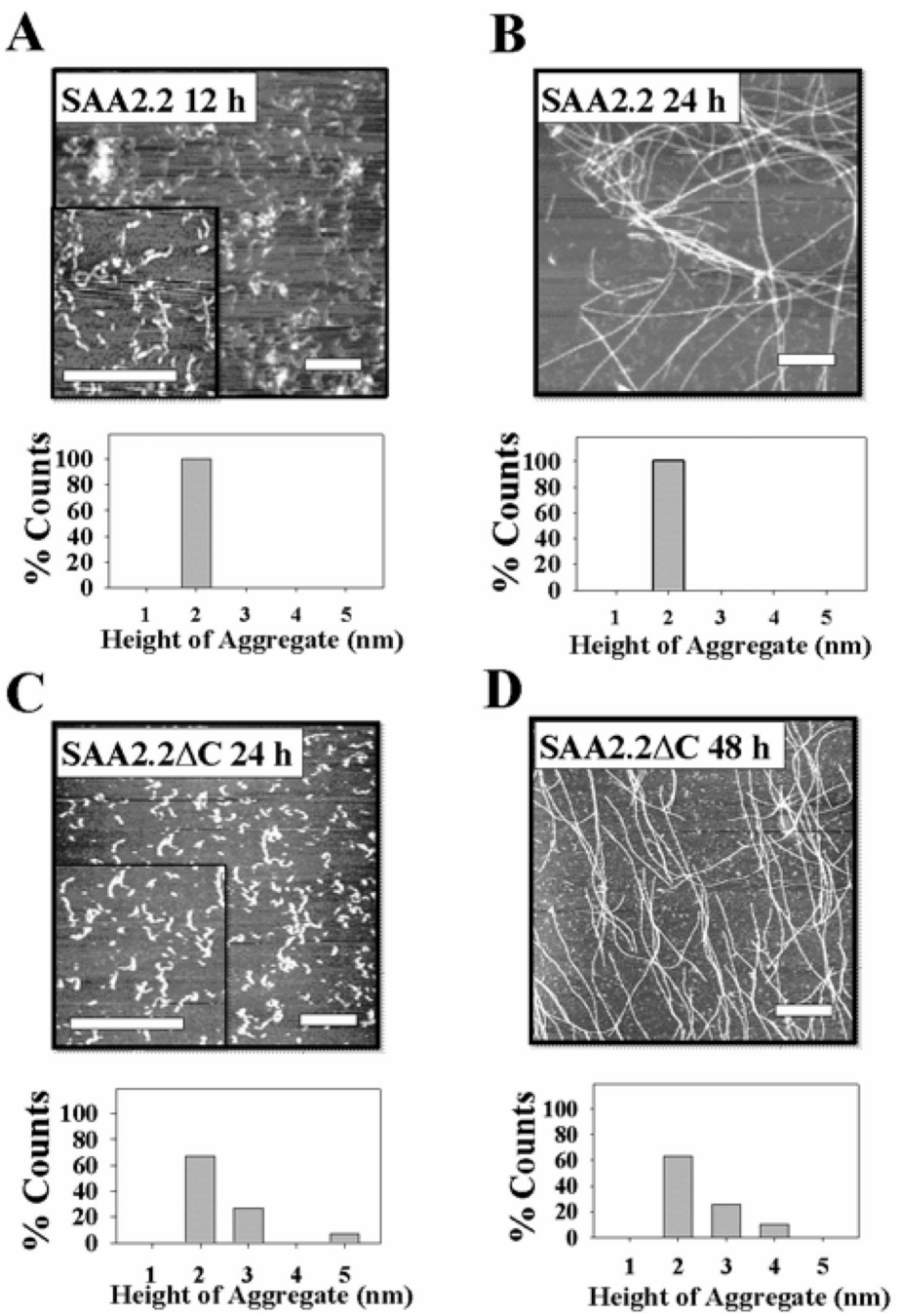

Figure 3.

AFM analysis and height distribution of aggregates formed by SAA2.2 and SAA2.2ΔC. (A) SAA2.2: 12 h, 37 °C; (B) SAA2.2: 24 h, 37 °C; (C) SAA2.2ΔC: 24 h, 37 °C; and (D) SAA2.2ΔC: 48 h, 37 °C. All scale bars represent 1 μm.

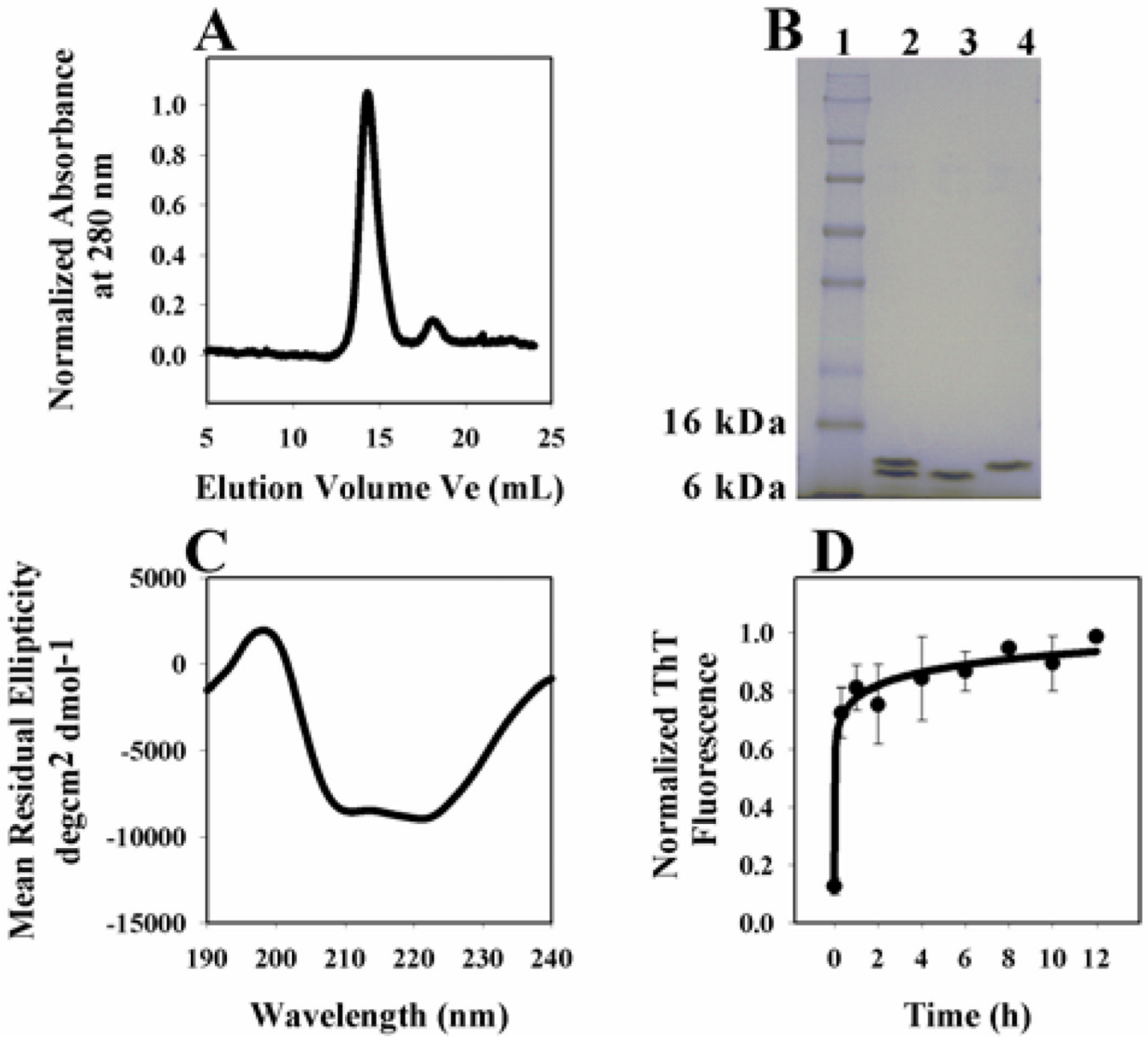

Figure 4.

Characterization of the structure and aggregation of the "co-oligomer" obtained by refolding an equimolar mixture of SAA2.2 and SAA2.2ΔC. (A) Size exclusion chromatography elution profile of the "co-oligomer". (B) SDS-PAGE gel; lane 1: protein ladder, lane 2: "co-oligomer", lane 3: SAA2.2ΔC, and lane 4: SAA2.2. (C) Far UV-CD spectrum of the "co-oligomer". (D) ThT fluorescence assay results to monitor the fibrillation of the "co-oligomer". The concentration of the protein was 30 μM. SEC and CD experiments were performed at 4 °C. ThT fluorescence intensities were recorded by incubating the samples at 37 °C.

Table 1

Oligomeric State of SAA and SAA2.2ΔC at 4 °C and 37 °C.

		Aggregation at 37 °C		
Protein	**Oligomeric state upon refolding at 4 °C (Figure 1)**	**Time to reach plateau in aggregation kinetics curve (Figure 2)**	**Predominant species present after 24 h (Figure 3)**	**Predominant species present after 48 h (Figure 3)**
SAA2.2	Octamer	0.5 h	Fibrils	Fibrils
SAA2.2ΔC	HMW aggregate (70–170 mer)	16 h	Protofibrils	Fibrils